Solar-Terrestrial Physics. 2023. Vol. 9. Iss. 4. P. 3–16. DOI: 10.12737/stp-94202301. © 2023
M.B. Krainev, G.A. Bazilevskaya, M.S. Kalinin, V.V. Mikhailov, A.K. Svirzhevskaya, N.S. Svirzhevsky. Published by INFRA-M Academic Publishing House

UDC 524.1
DOI: 10.12737/stp-94202301

Received July 03, 2023
Accepted September 05, 2023

FIFTY YEARS OF STUDYING THE GCR INTENSITY DURING INVERSION OF HELIOSPHERIC MAGNETIC FIELDS I. OBSERVATIONS

M.B. Krainev
Lebedev Physical Institute RAS,
Moscow, Russia, mkrainev46@mail.ru

G.A. Bazilevskaya
Lebedev Physical Institute RAS,
Moscow, Russia, gbaz@rambler.ru

M.S. Kalinin
Lebedev Physical Institute RAS,
Moscow, Russia, kalininms@lebedev.ru

V.V. Mikhailov
Moscow Engineering-Physics Institute,
Moscow, Russia, vvmikhajlov@gmail.com

A.K. Svirzhevskaya
Lebedev Physical Institute RAS,
Moscow, Russia, svirzhevskayaak@lebedev.ru

N.S. Svirzhevsky
Lebedev Physical Institute RAS,
Moscow, Russia, svirzhevskyns@lebedev.ru

Abstract. The effects of the 22-year variation of solar magnetic fields in the galactic cosmic ray (GCR) intensity were first observed and interpreted as manifestations of inversion of the high-latitude solar magnetic field in properties of heliospheric magnetic fields by the Lebedev Physical Institute team in 1973. Since then, these effects have been studied already for 50 years.

The situation with the heliospheric magnetic field is clear for periods of medium and low sunspot activity — the heliosphere consists of two unipolar "hemispheres" separated by a wavy global heliospheric current sheet and characterized by a general polarity *A* (unit quantity with the sign of the radial component of the heliospheric magnetic field in the northern "hemisphere"). Yet there is no consensus on what the inversion of the heliospheric magnetic field is and which effects in the GCR intensity are connected with this phenomenon.

In this article, we briefly formulate general concepts of the 22-year variation in characteristics of the Sun, heliosphere, and GCR intensity and discuss the observed effects in the GCR intensity, which we attribute to the heliospheric magnetic field reversal. Models for this phenomenon and the results of GCR intensity calculations with these models will be discussed in the next article.

Keywords: heliosphere, heliospheric magnetic fields (HMF), inversion of HMF, galactic cosmic rays (GCR), GCR modulation, long-term GCR variations, 22-year GCR intensity variation, GCR during HMF inversion.

LIST OF ABBREVIATIONS

GCRs — galactic cosmic rays.

HMF — heliospheric magnetic field.

HCS — heliospheric current sheet.

CR — Carrington rotation.

SMFs — solar magnetic fields.

SC — solar cycle. So, for brevity, the solar cycle is designated in the SMF toroidal component (number, area, and other characteristics of sunspots, active regions, flares, coronal mass ejections, etc.). Synonyms are the 11-year solar cycle, the sunspot solar cycle.

EH — energy hysteresis in the GCR intensity.

RBM — regular balloon monitoring of cosmic rays — an experiment conducted by Lebedev Physical Institute RAS (LPI RAS) since 1957.

NM — cosmic ray neutron monitors.

PAMELA — A Payload for Antimatter Matter Exploration and Light-nuclei Astrophysics — cosmic ray detector on board the satellite Resource DK1.

AMS-02 — Alpha Magnetic Spectrometer – cosmic ray detector on board the International Space Station.

INTRODUCTION

Solar magnetic fields and their 22-year variations have been known for more than a hundred years since their discovery in bipolar groups of sunspots [Hale, 1908] and polar regions [Hale, 1913] and observation of changes in the polarity of the leading and following sunspots in a new cycle's sunspots [Hale et al., 1919]. To make it clearer what our article is about, Figure 1

presents observations of solar and heliospheric characteristics, and GCR intensity from 1955 onward.

According to the dynamo theory, there are two branches of solar magnetic fields (SMFs) with significantly different properties on the Sun [Charbonneau, 2010]. In the first approximation, high-intensity toroidal magnetic fields B_{tor} are associated with active regions and related phenomena (sunspots, flares, coronal mass ejections, etc.), and quantitative indices obtained from 150-year observations are the area S_{ss} and the position of sunspot groups (panels *a*, *b*). The SMF poloidal branch, which is weaker in intensity B_{pol}, is primarily linked to polar (high-latitude) quasi-radial fields opposite in direction at the north and south poles, and with coronal holes; the quantitative indices are the number of polar faculae observed for more than a hundred years [Sheeley, 2008], as well as the component along the line of sight of high-latitude SMFs, which has been regularly observed since 1976 (panel *c*). Activity of the two SMF branches develops in antiphase. Toroidal fields peak, of course, during a solar cycle (SC) maximum and change polarity shortly after minimum of this cycle. The poloidal branch is maximum at solar minimum and changes polarity at solar maximum. Thus, despite the SMF strength of each of the branches varies with ~11-year period, there is a ~22-year cycle in their polarity.

However, the modulation of galactic cosmic rays (GCRs) we are interested in occurs in the heliosphere (the outer layer of the solar atmosphere $r_{in}^{HS} \le r \le r_{out}^{HS}$, where $r_{in}^{HS} \approx 10\ r_{\odot}$ and $r_{out}^{HS} \ge 100$ AU) and is caused by the influence of the solar wind and heliospheric magnetic fields (HMFs) on charged particles (panel *d*). During most of SC in terms of the direction of regular HMF to the Sun (B_r<0) or from the Sun (B_r>0), the heliosphere consists of two oppositely directed unipolar hemispheres separated by a wavy global heliospheric current sheet (HCS) with a degree of waviness α_{qt} (panel *d*). Figure 1, *a*, *d* shows that both the HMF strength and the degree of HCS waviness correlate with the SMF toroidal branch. The above simple pattern of the two-hemisphere heliosphere is violated during SC maxima.

GCRs with isotropic intensity J and low anisotropy $\delta J/J$ penetrate into the heliosphere from the Galaxy region surrounding the Sun, are affected by the solar wind and HMF, and their characteristics change significantly (or are modulated). The GCR intensity is seen (panel *e*) to peak during SC minima and vice versa, i.e. in the first approximation it anticorrelates with the SMF sunspot cycle. The concept of the sunspot cycle as the only cause of the long-term GCR variation dominated during the first decades of the study of its modulation. Nonetheless, already during the development of the idea about the heliosphere as an outer extended layer of the Sun's atmosphere reflecting the processes occurring on its surface, it was suspected that there might be 22-year effects in GCR characteristics.

Such effects in the GCR anisotropy were first identified by S. Forbush in 1967–1969 from time variations in daily wave maximum in data from ionization chambers [Forbush, 1969]. The effect of variability of the solar general magnetic field (as MF in the polar regions of the photosphere was called then) on the GCR intensity was first detected by the LPI team in 1973 [Charakhchyan et al., 1973] and was interpreted as the effect of inversion of this field in HMF properties. Since then, the manifestations of the 22-year HMF cyclicity in the GCR intensity have been studied for fifty years, and attention has mainly been drawn to the phenomena occurring during low solar activity and hence two-hemispheric distribution of HMF polarity. Note that by the intensity in this paper is meant its isotropic part, and by anisotropy is implied a characteristic of the deviation of the exactly defined intensity from isotropy (in the simplest case, a vector).

Yet, for high sunspot activity and HMF inversion, there is no consensus on which effects in the GCR intensity are caused by this inversion, although for the period of regular monitoring of GCRs of different energies the HMF inversion has already occurred seven times. Moreover, in most studies on the GCR behavior during these periods (see, e.g., [Aslam et al., 2023]), individual GCR intensity effects typical for different HMF inversion periods are usually not distinguished. It would therefore be useful to discuss such effects regularly (as in [Charakhchyan et al., 1973; Svirzhevskaya et al., 1975]) identified for different HMF inversion periods in the LPI team's works.

While we analyze the GCR behavior during HMF inversion, to discuss this behavior in a modern light we should formulate the general concept of the 22-year cyclicity in heliospheric characteristics and GCR intensity. We first, therefore, briefly formulate general facts and ideas about the 22-year variations in SMF and HMF, as well as in GCR intensity (Section 1). Then, we discuss the observed effects in the GCR intensity, which we associate with HMF inversion (Section 2). The results are discussed in Section 3. Simulation of heliospheric characteristics and GCR intensity during HMF inversion will be examined in the next article.

1. GENERAL FACTS AND IDEAS ABOUT 22-YEAR VARIATIONS IN THE HELIOSPHERE

Characteristic dimensions of toroidal SMFs (for example, a distance between leading and following sunspots) L_{tor} are small compared to the solar radius $r_{\odot}$, $L_{tor} << r_{\odot}$, whereas characteristic dimensions of poloidal SMFs (approximately the diameter of the photosphere) $L_{pol} \approx r_{\odot}$. Due to the layer $r_{\odot} \le r \le r_{in}^{HS}$ between the photosphere and the heliosphere in which the main energy factor is the magnetic field, when SMF penetrates into the heliosphere, where the solar wind kinetic energy forms the basis of the energy balance, larger-scale poloidal SMFs gain a great advantage [Schatten et al., 1969; Altschuler, Newkirk, 1969]. At the same time, they are significantly affected by powerful toroidal fields, possibly due to the heating of the corona and the associated system of horizontal currents [Zhao, Hoeksema, 1994].

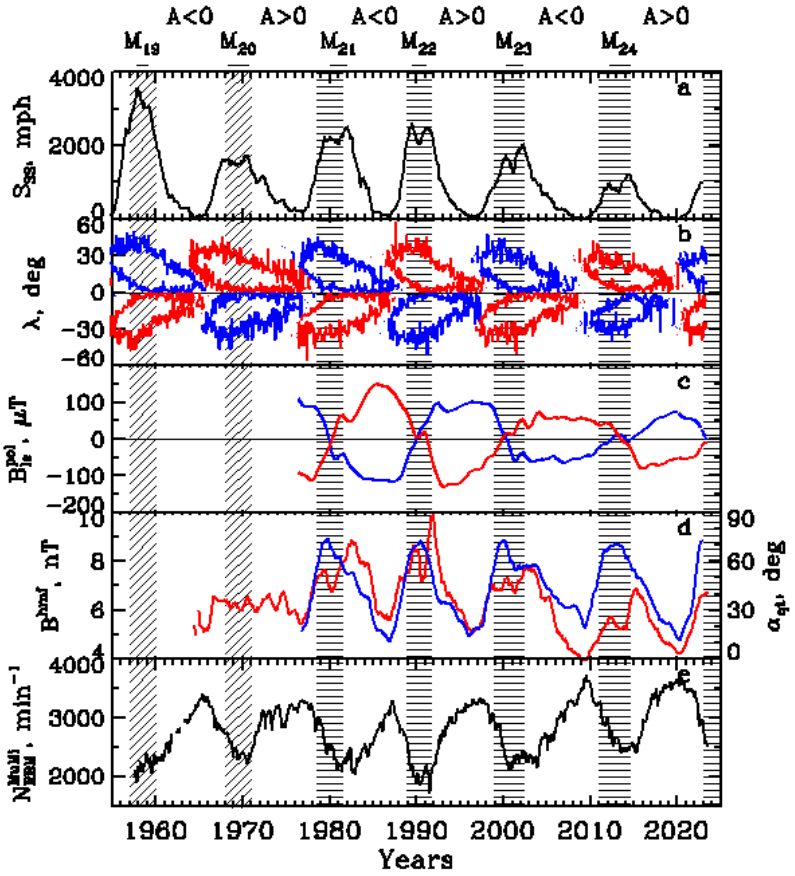

Figure 1. Long-term variations in solar and heliospheric magnetic fields and GCR intensity in 1955–2023. The periods of maximum sunspot activity (the time interval between two Gnevyshev peaks [Gnevyshev, 1967; Storini et al., 2003]) and the overall HMF polarity *A* are shown above the top panel; hatched bands are HMF inversion periods. Horizontal hatching indicates the periods for SC 21–24 in accordance with [Krainev, 2019] and the period of HMF inversion in SC 25, which began in Carrington rotation (CR) 2265 at the end of 2022 [http://wso.stanford.edu]; oblique hatching, those observed in individual measurements of SMF, but before its regular scanning. The solar and heliospheric characteristics (except for latitudinal boundaries of sunspot groups) are smoothed with a period of ~1 year. Panels *a*, *b* are the area of sunspot groups and the latitudinal boundaries of sunspot groups with B_φ>0 (blue lines) and B_φ<0 (red lines) [https://solarscience.msfc.nasa.gov; ftp://ftp.swpc.noaa.gov/pub/forecasts/SRS]. In panel *c* is SMF component along the line of sight from Earth in the northern (blue line) and southern (red line) polar regions of the solar photosphere [http://wso.stanford.edu]. In panel *d* is the HMF radial component modulus in the Earth orbit (red line) [ftp://omniweb.gsfc.nasa.gov/pub/data/omni/low_res_omni] and the degree of HCS waviness α_{qt} (blue line) [http://wso.stanford.edu]. Panel *e* is the monthly average rate of the Geiger—Müller counter at the Regener—Pfotzer maximum as derived from the RBM experiment in the Murmansk Region and Antarctica [https://sites.lebedev.ru/en/DNS_FIAN]

As a result, despite the HMF strength correlates with the toroidal SMF characteristics, it is topologically the poloidal SMFs that form HMF in the form of two unipolar hemispheres of opposite polarity separated by wavy global HCS. Such a representation related to the period outside the poloidal SMF inversion had already developed by the mid-1970s [Shulz, 1973] and is characterized by the overall HMF polarity *A* (a unit quantity with the sign of the HMF radial component B_r in the northern hemisphere of the heliosphere) and by the degree of HCS waviness (quasi-tilt α_{qt} — half of the latitude range occupied by HCS). Note that we separate the observed characteristic (quasi-tilt α_{qt}), determined for each CR from the results of SMF scanning at the Wilcox Solar Observatory (WSO), and tilt (tilt of a current sheet) α_t — the parameter of the model of the so-called tilted current sheet [Jokipii, Thomas, 1981] assuming that the current sheet at a fixed distance is in a plane tilted to the equator by an angle α_t. The HMF inversion, i.e. reversal of its polarity *A*, occurs during SC maximum and is likely to be associated with the change of old fields for new ones on the Sun due to the poleward drift of remnants of toroidal fields [Charbonneau, 2010]. Because of insufficient information on the heliosphere, WSO data [http://wso.stanford.edu], obtained from daily scanning of photospheric SMFs, is very important for a quantitative representation of HMF in the entire heliosphere. Qualitative ideas about HMF during its inversion are discussed below. In Figure 1, horizontal hatching for SC 21–24 according to regular WSO measurements and our model (see below) shows the inversion periods tabulated in [Krainev, 2019]; and for current SC 25, the HMF inversion period that began at the end of 2022 (CR 2265). Oblique hatching indicates the HMF inversion periods in SC 19–20 according to measurements of high-latitude SMFs [Babcock, 1959; Howard, 1974;

Sheeley, 1976], when regular scanning and processing of SMFs at WSO (since 1976) did not begin yet.

The concepts of mechanisms behind the influence of HMF ordered distribution on GCRs during periods outside of its inversion were, for the most part, formulated in the 1970s–1980s: 1) particle drift in an inhomogeneous magnetic field ([Jokipii et al., 1977]; effects depend on the sign of qA (we will denote such a dependence as $\sim qA$), where q is the particle charge); 2) particle diffusion in terms of the helicity of regular HMF ([Bieber et al., 1987]; $\sim A$ effects); possibly 3) reconnection between HMF and the galactic field ([Schatten, Wilcox, 1969; Nagashima, 1977; Ahluwalia, 1979]; $\sim A$ effects), and 4) manifestation of the electric potential difference between the heliosphere and interstellar space ([Krainev, 1979; Jokipii, Levy, 1979]; $\sim qA$ effects). At the same time, the corresponding observed effects were discovered in the GCR intensity [Jokipii, Thomas, 1981]: alternation of peak- and plateau-shaped time profiles of the intensity of GCR nuclei during periods $A<0$ and $A>0$ respectively (see Figure 1, *e*).

Due to the theoretical description of GCR behavior, an opinion was formed [Potgieter, 2013] about the magnetic drift as an important mechanism of GCR modulation near SC minima when the degree of HCS waviness is low (quasi-tilt $\alpha_{qt}<30°$). We assign the remaining part of SC ($\alpha_{qt}>30°$, about half or most of SC depending on the α_{qt} model) to the period when the HMF inversion can be important for GCRs. Note that already in the first work [Jokipii, Thomas, 1981] in which the effect of alternating peak- and plateau-shaped time profiles of GCR intensity depending on the overall HMF polarity and the particle charge was obtained from calculations and confirmed by observations, the authors limited their conclusion to the time period when $\alpha_t<30°$ because in periods closer to SC maximum, as they said, the entire structure of the magnetic field changes sign and we cannot expect a simple ordered structure predicted for the periods of forthcoming solar minimum. Thus, the periods when we can expect an effect of HMF inversion on the GCR intensity comprise 1) a short period (less than a year) of a rapid intensity decrease before the start of HMF inversion; 2) the HMF inversion per se when a transition occurs from the overall HMF polarity $A<0$ to $A>0$ or vice versa (inversion of these types can also be referred to as inversions with $dA/dt>0$ or $dA/dt<0$); 3) the initial period of intensity increase after HMF inversion (~2 years). Since the HMF inversion until it begins cannot have an effect on the GCR intensity, the GCR behavior in the first of these periods will not be analyzed.

As for the HMF inversion structure, our qualitative ideas of it as consisting of three phases were formed about ten years ago [Krainev, Kalinin, 2014; Krainev et al., 2015; Krainev, 2019]. Almost throughout SC, HMF before inversion is divided into two unipolar hemispheres of opposite polarity with an overall polarity A_1, separated by single and global (i.e. connecting all longitudes) HCS. In the first phase of the inversion (we call it pre-inversion), besides this global HCS there are additional opposite polarity HMF islands in the unipolar hemispheres, i.e. HCS losses its uniqueness, but retains its global character. The pre-inversion phase is followed by the phase of the HMF inversion per se when HCS loses its global character, i.e. during some solar rotations there are no HCS connecting all longitudes. Finally, during the third phase of HMF inversion (post-inversion), HCS again assumes a global character corresponding to the new overall polarity $A_2 = -A_1$, opposite to the original one, but there is no single HCS yet. Finally, after the entire inversion, an HMF is established with two opposite polarity unipolar hemispheres with A_2, which are separated by single global HCS. Note that the HCS shape is defined by WSO models [http://wso.stanford.edu] as a shape of neutral lines of the radial magnetic field on the HMF source surface. It is believed that extending this structure to the heliosphere by the radial solar wind in view of solar rotation gives a good approximation to the observed shape of HCS [Burton et al., 1994; Smith, 2001, 2011]. The time limits of the three HMF inversion phases for the last four cycles (SC 21–24), listed in Table in [Krainev, 2019], as well as the beginning of HMF inversion for SC 25 (Figure 1), have been determined using the classical WSO model version and change slightly for another (radial) version. As mentioned in Introduction, quantitative modeling of heliospheric characteristics and GCR intensity during HMF inversion will be discussed in the next article.

2. PHENOMENA OBSERVED IN GCR INTENSITY DURING HMF INVERSION

By the early 1970s, systematic monitoring of GCR intensity (mainly protons of rather high kinetic energy $T \geq 1$ GeV) on the surface and in Earth's atmosphere had been carried out for more than 30 years: ionization chambers since 1936 [Forbush, 1939]; separate neutron monitors (NM) since 1952 [Simpson, 1985, 2000]; worldwide NM network [http://www.nmdb.eu], and regular balloon monitoring (RBM) [https://sites.lebedev.ru/en/DNS_FIAN] since 1957. Direct extraterrestrial measurements of GCRs of other types (nuclei, electrons, etc.) and lower-energy protons began in the 1960s, but until the mid-2000s monitoring of their intensities in a wide range of energies was irregular [Evenson et al., 1983; Garcia-Munoz et al., 1986].

From the results of monitoring made by Forbush already in 1954, an overall anticorrelation was found between the GCR nuclear component intensity and SC [Forbush, 1954]. For the first two decades, data analysis involved comparing time variations in GCR intensity with the behavior of various SC characteristics and with episodic satellite observations. During those years, general concepts of the heliosphere were developed [Parker, 1963], foundations of the GCR modulation theory were formed [Parker, 1958; Krymskiy, 1964; Parker, 1965], the coefficients of the transport equation were estimated by measuring heliospheric characteristics.

Although, as already indicated in Introduction, in the 1950s and 1960s, the long-term GCR variations were mainly associated with 11-year SC, the 22-year cyclicity of both SMF branches had long been known from direct measurements of strong magnetic fields of sunspots and weak fields in polar regions. Therefore, when analyzing

data on GCR characteristics, the possibility of the 22-year cyclicity of SMF in the data should have been taken into account.

The first such manifestation was a 22-year wave in GCR anisotropy, discovered by Forbush, when analyzing data from ionization chambers, from the time of daily wave maximum [Forbush, 1969]. Let us take a closer look at the history of the discovery of manifestation of the SMF 22-year cyclicity in GCR intensity. Furthermore, since we use the RBM experiment data, note that within the framework of this experiment, conducted by LPI since 1957, a balloon probe transmits a pulse to a receiver when each particle of the ionizing component of primary and secondary cosmic rays passes through a detector (Geiger—Müller counter). Such measurements are regularly performed at several ground stations (currently three times a week in the Murmansk and Moscow regions and at Mirny Observatory in Antarctica). Below, when discussing the effects observed in the GCR intensity, we use the monthly average combined count rate of the RBM detector $N_{\mathrm{RBM}}^{\mathrm{MuMi}}$ from Murmansk and Mirny data in the maximum dependence of the count rate on the amount of matter above the device (Regener—Pfotzer maximum). The count rate $N_{\mathrm{RBM}}^{\mathrm{MuMi}}$ correlates with the intensity of protons having a kinetic energy T>0.1 GeV [Stozhkov et al., 2007], the effective energy $T_{\mathrm{eff}}^{\mathrm{MuMi}}$ ≈3–5 GeV. The RBM experiment is described in more detail in [Bazilevskaya, Svirzhevskaya, 1998; Stozhkov et al., 2009] and on the website [https://sites.lebedev.ru/en/DNS_FIAN]. Hereinafter, we call the count rate $N_{\mathrm{RBM}}^{\mathrm{MuMi}}$ the RBM count rate; and the monthly average count rate of the Moscow neutron monitor $N_{\mathrm{NM}}^{\mathrm{Mo}}$, NM data (effective energy $T_{\mathrm{eff}}^{\mathrm{NM}}$ ≈10 GeV).

When comparing time profiles of SC characteristics and GCR intensity from RBM experiment and NM data for 1957–1968. [Stozhkov, Charakhchyan, 1969; Stozhkov, Charakhchyan, 1970], it was observed that the time profile of the detector count rate $N(t)$ is well approximated by expressions

$$N(t) = N_0 \exp\left(-C\psi(t)\right), \quad (1)$$

$$\psi = \eta^{0.8}\,\lambda^{-1.2}, \quad (2)$$

where ψ is the modulating factor; η, λ are the monthly average number of sunspot groups on the disk and the average solar latitude modulus of these sunspot groups [https://solarscience.msfc.nasa.gov]; N_0, C are the constants depending on the energy of detected particles, with N_0 implying the count rate at ψ=0 unmodulated by solar activity. Figure 2 compares the behavior of the count rate $N_{\mathrm{RBM}}^{\mathrm{MuMi}}$ and N at N_0 and C, determined from the linear regression of $\ln N_{\max}^{MuMi}(t)$ and ψ(t) for the period between HMF inversions in SC 19 and 20 (1960–1968). The RBM data behavior is seen to be well approximated by expressions (1), (2) (correlation coefficient ρ=0.91 ±0.02 for a series length N=87).

Nonetheless, after the maximum of SC 20 since 1971, the observed RBM count rate sharply went up, whereas the count rate expected from the behavior of the factor ψ increased at about the same rate as in the early 1960s. Charakhchyan et al. [1973] compared this fact with the data on the high-latitude SMF inversion during SC 19 in 1957–1958 [Babcock, 1959] and with the inversion expected approximately every 11 years [Babcock, 1961]. This is due to the expected inversion in SC 20, caused by the weakening of the solar magnetic dipole and hence, as with the terrestrial dipole, the HMF cutoff rigidity. Now, when it became clear that the concept of cutoff rigidity is not applicable to the heliosphere, we attribute the above effect of the discrepancy between the observed GCR intensity in the early 1970s and the expected approximation of observations for the 1960s to the varying shape of the time profile of the GCR intensity for periods with A<0 and A>0 and to the transition from a cycle with a slow recovery of proton intensity after SC maximum (qA< for protons in the 1960s) to a cycle with a rapid increase (qA>0 for protons in the 1970s). We therefore consider the significant difference in the rate of intensity recovery after maxima with HMF inversion with dA/dt<0 and dA/dt>0 to be the first effect in the GCR intensity behavior associated with the HMF inversion. Note that attention was first drawn to the 22-year periodicity in the rate of intensity recovery after SC maxima by Ahluwalia [1979].

The behavior of the RBM count rate (see Figure 2) is compared with its approximation according to (1), (2) not only for the above 22-year period between the HMF inversions in SC 19 and 21 (1960–1978) with N_0 and C determined for the period with the overall HMF polarity A<0 between the HMF inversions in SC 19 and 20 (1960–1968), but also for the next two 22-year periods (1982–1999 and 2002–2022) with N_0 and A defined for the periods with A<0. The observed behavior of the RBM count rate in the 1980s is seen to be approximated by (1), (2) worse than in 1960 (ρ=0.83 ±0.03 at N=87), although there is a significant excess of the observed GCR intensity over the expected one according to (1), (2) a year after the end of the HMF inversion. The deterioration of the approximation is likely to be due to the very acute time profile of the observed intensity in the 1980s such that other exponents for (2) are required for its approximation [Bazilevskaya et al., 1995]. Nevertheless, for the last 22-year period (2002–2022) the situation is close to that observed in 1960–1978: a good approximation of observations in the period with A<0 (ρ=0.90 ±0.02 at N=101) and a systematic (albeit small) excess of the observed intensity over the approximation by (1), (2) after the inversion period with dA/dt>0.

In order to emphasize more strongly the difference between the time profiles of the intensity of nuclei in periods with A<0 and A>0, Figure 3 illustrates regression between the RBM count rate and its time derivative (or the rate of change in the count rate) for the same three 22-year periods with approximately the same rate. On the contrary, during periods with A>0, the RBM count rate first increases rapidly in the range 500–700 $\mathrm{min}^{-1}\cdot\mathrm{month}^{-1}$, then the rate of its change decreases sharply, remaining low for some time after reaching maximum. In general terms, the described behavior of the RBM count rate and its time derivative corresponds

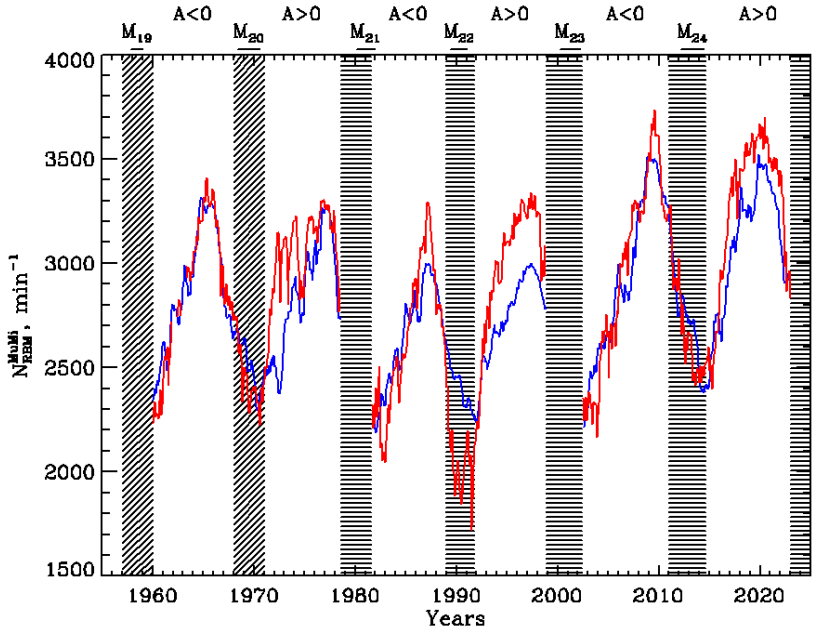

Figure 2. Time profiles of monthly average RBM count rate (red line) and its approximation by (1), (2) for periods with $A<0$ (blue line) for three 22-year cycles. The designations above the panel and the hatched bands are the same as in Figure 1

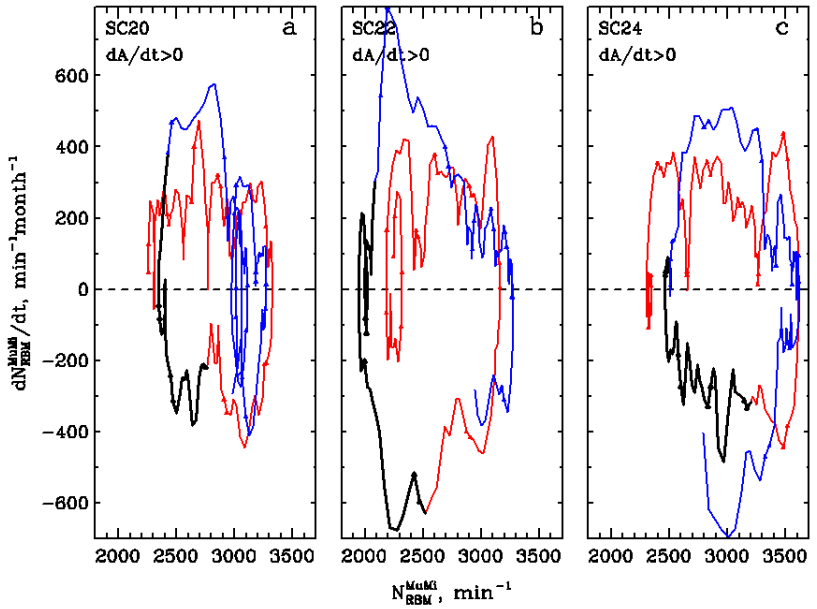

Figure 3. Regression between monthly average RBM count rate, smoothed by 13 points, and its time derivative for three 22-year periods centered on HMF inversion periods with $dA/dt>0$ in SC 20 (*a*), SC 22 (*b*), and SC 24 (*c*). Red curves are periods with $A<0$; blue curves, those with $A>0$; black bold curves, an HMF inversion period

to a relatively slow recovery of proton intensity after SC maximum with an acute time profile of the intensity of nuclei in periods with $A<0$; and at $A>0$, to a faster increase in intensity after inversion with a relatively flat profile around the intensity maximum [Jokipii, Thomas, 1981].

Almost simultaneously with the above effect of a significant excess of the observed intensity over its approximation by (1), (2) after the HMF inversion in 1969–1971, the second effect in the behavior of GCR intensity was linked to the HMF inversion — a sharp change in the energy dependence of the long-term GCR variation during the HMF inversion [Svirzhevskaya et al., 1975]. This effect is broadly termed as energy hysteresis (EH) because of the fact that a loop, which outwardly resembles a loop of magnetic hysteresis, is formed on plots of the regression between GCR intensities of low (e.g., recorded in the RBM experiment) and high (e.g., detected by NM) energies due to this sharp change in the energy dependence. Note that hysteresis in the GCR intensity is also often applied to the effects in comparing the intensity and solar activity characteristics (see, e.g., [Simpson, 1963]). We will refer to the effect in comparing intensities of differently charged particles as charge hysteresis (see below).

In fact, the sharp change in the energy dependence of the long-term GCR modulation during maximum of

SC 20 was observed in [Lockwood et al., 1972; Burger, Swanenburg, 1973] earlier than in [Svirzhevskaya et al., 1975]. Nevertheless, although Lockwood et al. [1972] attributed this phenomenon to a strong Forbush effect in June 1969, Svirzhevskaya et al. [1975] considered it as a manifestation of HMF inversion during this period. In Figure 4 illustrating this phenomenon, the behavior of the count rate in the RBM experiment is compared with the Moscow NM count rate, reduced to $N_{\mathrm{RBM}}^{\mathrm{MuMi}}(t)$ by the linear regression for the periods between HMF inversions (for the periods of the 1960s, 1970s, 1980s, 1990s, 2000s, and 2010s, the correlation coefficients are, respectively, ρ=0.987 ±0.003 (N=87), 0.82 ±0.04 (N=90), 0.985 ±0.003 (N=87), 0.984 ±0.003 (N=84), 0.971 ±0.006 (N=101), 0.980 ±0.004 (N=100)). The difference between the RBM count rate and the Moscow NM count rate, reduced to $N_{\mathrm{RBM}}^{\mathrm{MuMi}}(t)$ for the previous period between HMF inversions, during HMF inversion characterizes a change in the energy dependence of the long-term GCR modulation during SC maximum. We can see (Figure 4) that a really sharp change in the energy dependence of the GCR long-term modulation for the pair of RBM and Moscow NM is observed only for the HMF inversion in SC 20 (1969–1972), with which this effect was associated [Svirzhevskaya et al., 1975], and in SC 24 (2012–2014). In the rest of the HMF inversion periods in SC 21–23, the difference between the RBM count rates and the Moscow NM count rate, reduced to $N_{\mathrm{RBM}}^{\mathrm{MuMi}}(t)$ for the previous HMF-inversion-free period, is insignificant, i.e. there was no sharp change in the energy dependence of the long-term GCR modulation during the HMF inversion periods in these solar cycles.

Another format in which EH is usually visualized is the regression relationship between count rates of detector of GCRs having different energies, in particular RBM and NM experiments. Figure 5 shows these relationships for the 22-year periods centered on the inversion periods of SC 20–24. There is a sharp change in the energy dependence of the long-term GCR modulation during the HMF inversion in SC 20 and a large EH loop for the corresponding 22-year period. There are also local loops during maximum intensity of all the cycles, which arise from the difference between kinetic properties (first of all, diffusion coefficients and magnetic drift velocity) of particles of different energies. As for the periods of GCR intensity minima that occur during sunspot maxima and HMF inversion, SC 20 and 24 again stand out by the scale of the change in the energy dependence of the GCR modulation, but the latter without a significant EH loop.

Both HMF inversion periods with a relatively sharp change in the energy dependence of the long-term GCR modulation (in SC 20 and 24) are the periods with dA/dt >0, i.e. they are characterized by a transition from the overall HMF polarity A<0 to A>0. It is interesting to detail this effect for differential intensities of primary GCRs (or for mean intensities in fixed ranges of energy or rigidity), and not only for the integral intensities of a mixture of primary and secondary particles recorded in the RBM and NM experiments.

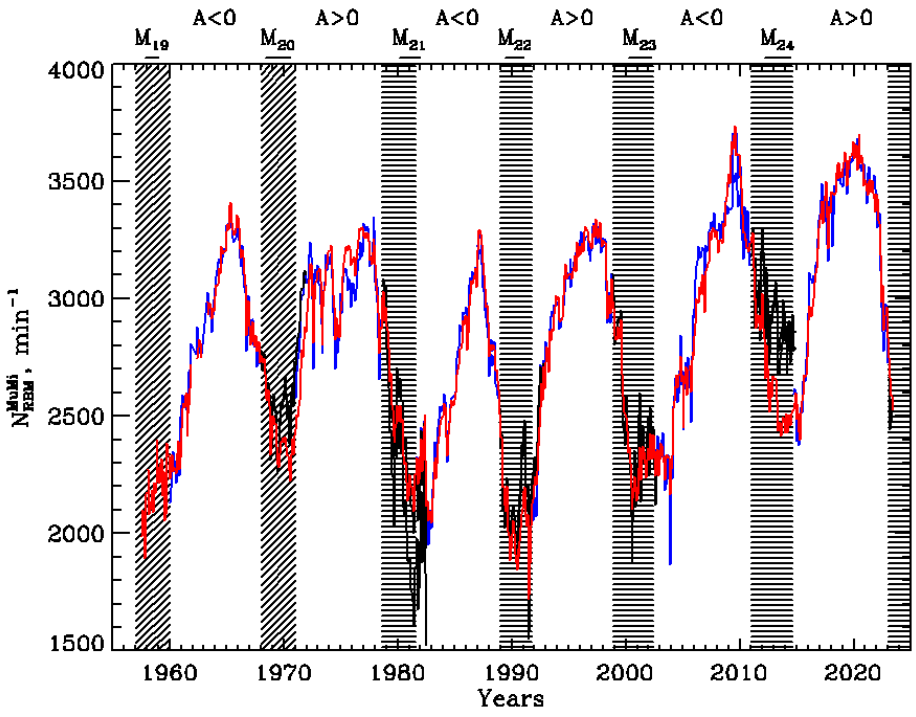

Figure 4. Time profile of RBM detector count rate (red curve) versus Moscow NM count rate, reduced to $N_{\mathrm{RBM}}^{\mathrm{MuMi}}(t)$ by linear regression for the periods between HMF inversions (blue curve). The designations above the top panel and the hatched bands are the same as in Figures 1, 2. Black curves indicate extrapolation of the reduced Moscow NM count rate, determined from the previous period between inversions, for an HMF inversion period

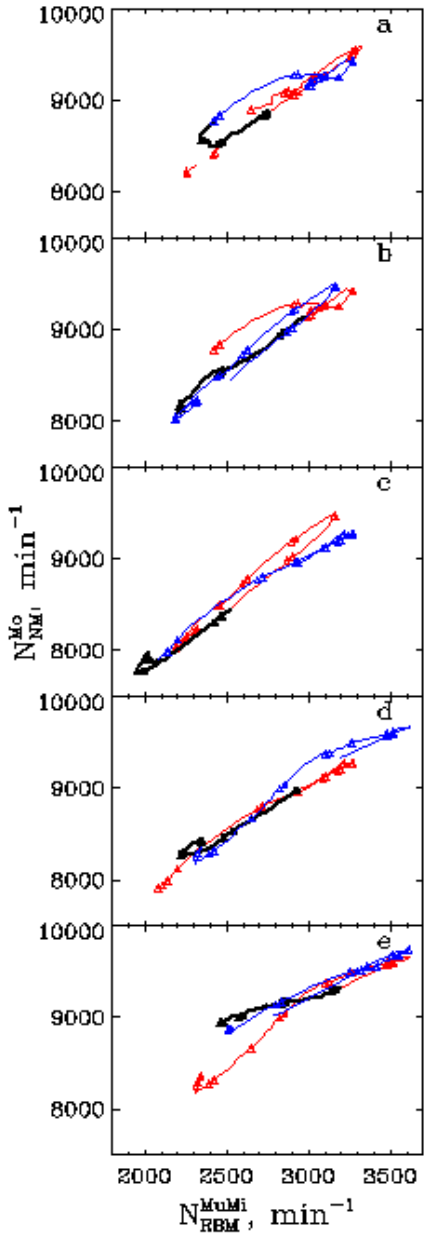

Figure 5. Regression between RBM and Moscow NM detectors' monthly average count rates, which are smoothed by 13 points, for 22-year periods centered on the HMF inversion periods in SC 20 (*a*), SC 21 (*b*), SC 22 (*c*), SC 23 (*d*), and SC 24 (*e*). Red lines are periods with $A<0$; blue, with $A>0$; black bold lines are HMF inversion periods. Triangles mark the beginning of each year

There were no reliable systematic measurements of differential intensities in wide energy ranges in the period around the HMF inversion in SC 20 (1968–1971), but in the period around the HMF inversion in SC 24 (2011–2014) the experiments PAMELA in 2006–2016 (see [Adriani et al., 2013; Martucci et al., 2018]) and AMS-02 from 2011 to the present (see [Aguilar et al., 2018, 2021]) provide such an opportunity.

For this purpose, series of proton intensities in rigidity ranges ~1–2, 2–3, 3–7.5 GV, averaged over Carrington or Bartels rotations for June 2006–February 2014 (PAMELA) and May 2011–2019 (AMS-02), have been formed from PAMELA [Martucci et al., 2018] and AMS-02 [Aguilar et al., 2018] data; as well as electron intensity series in approximately the same rigidity ranges and with the same time resolution, from AMS-02 data for May 2011–2017 [Aguilar et al., 2021]. Figure 6 exhibits time profiles of these intensities for 2006–2019.

To the data we have applied the procedure described above for the analysis of EH based on RBM and NM data. The proton intensities in the 2–3 and 3–7.5 GV rigidity ranges were reduced to the intensity in the 1–2 GV range by linear regression at certain time intervals, and then they were extrapolated to the HMF inversion period. The results are presented in Figure 7 as obtained by PAMELA (*a*) and AMS-02 (*b*).

Note that the HMF inversion period of interest is asymmetric with respect to the periods of available PAMELA and AMS-02 data. Unfortunately, there is no data for PAMELA for most 2010, and data for 2015 when, according to AMS-02 data (as well as RBM and NM data), the proton intensity rapidly recovered, has not been published. Most PAMELA data (for 2006–2012) refers to the period with the overall HMF polarity $A<0$ to the inversion period ($N=62$), for which we have made the main regression of the high-energy proton intensity to the low-energy intensity ($\rho=0.990\pm0.002$, 0.94 ± 0.01 between the intensities of respectively the second and third rigidity ranges to the intensity of the first range) and their time extrapolation to the HMF inversion period. The results of the auxiliary regression for a short interval $N=12$, shown by the dotted line, differ little from the results of the main regression ($\rho=0.95\pm0.03$, 0.87 ± 0.07).

Most AMS-02 data (for 2015–2019) relates to the period with the overall HMF polarity $A>0$ after the HMF inversion period ($N=65$) for which the main regression of the high-energy proton intensity to the low-energy intensity and their backward extrapolation to the same period were made. The corresponding correlation coefficients $\rho=0.990\pm0.002$, 0.975 ± 0.006, i.e. the linear regression between the intensities of low- and higher-energy protons is good. The AMS-02 data is available only since May 2011, we can therefore estimate the change in the energy dependence from the data for the period from $A<0$ to the inversion period in order to make a forward extrapolation of the normalized intensity for the HMF inversion period per se only for a very short interval 05.2011–2012 ($N=9$). Accordingly, the correlation coefficients at regression for this short (auxiliary) period are low, $\rho=0.8\pm0.1$, 0.6 ± 0.2. A significant violation of the energy dependence of variations during the HMF inversion (Figure 7, *b*) is clearly seen for forward extrapolation of reduced intensities to the HMF inversion period and is much less pronounced for backward extrapolation.

Using AMS-02 data [Aguilar et al., 2021], we can examine EH for electrons as well as the dependence of the HMF-inversion related effects on particle charge. To do this, for series of electron intensities in the 1–2, 2–3, 3–7.5 GV rigidity ranges, averaged over Bartels rotations for 05.2011–2017, we have used the procedure described above for the analysis of EH from RBM and

Moscow NM data, as well as from the proton intensity obtained by PAMELA and AMS-02. The correlation coefficients between the electron intensities of low and higher rigidities for the main regression period (N=31) ρ=0.993±0.002, 0.981±0.007; and for the short auxiliary period (N=9), ρ=0.8±0.1, 0.5±0.3. EH derived from electron data is depicted in Figure 8, *a*. Just as for protons, according to the AMS-02 electron data, a change in the energy dependence of long-term GCR variations is clearly seen in forward extrapolation of reduced intensities to the HMF inversion period and much less pronounced in backward extrapolation.

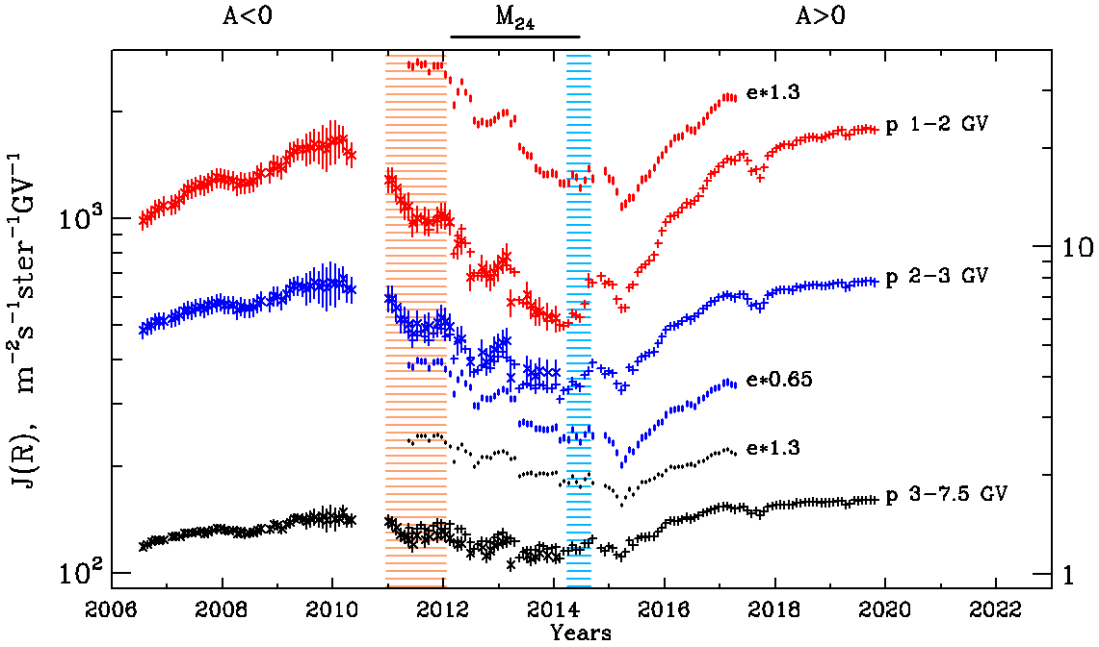

Figure 6. Time dependence of proton and electron intensities as derived from PAMELA and AMS-02 experiment data for 2006–2019. Periods of maximum sunspot activity (time interval between two Gnevyshev peaks [Gnevyshev, 1967; Storini et al., 2003]) and the overall HMF polarity *A* are shown above the top panel, and the hatched bands mark the HMF inversion period structure (pink band is pre-inversion; blue, post-inversion, and the period of the HMF inversion per se between them is not hatched [Krainev, 2019]). The scale along the left Y-axis corresponds to the proton intensity; along the right one, to the electron intensity. Red curves represent intensities of protons and electrons with 1–2 GV rigidity; blue, with 2–3 GV; black, with 3–7.5 GV. For electrons, intensities are multiplied by the coefficients given near the curves

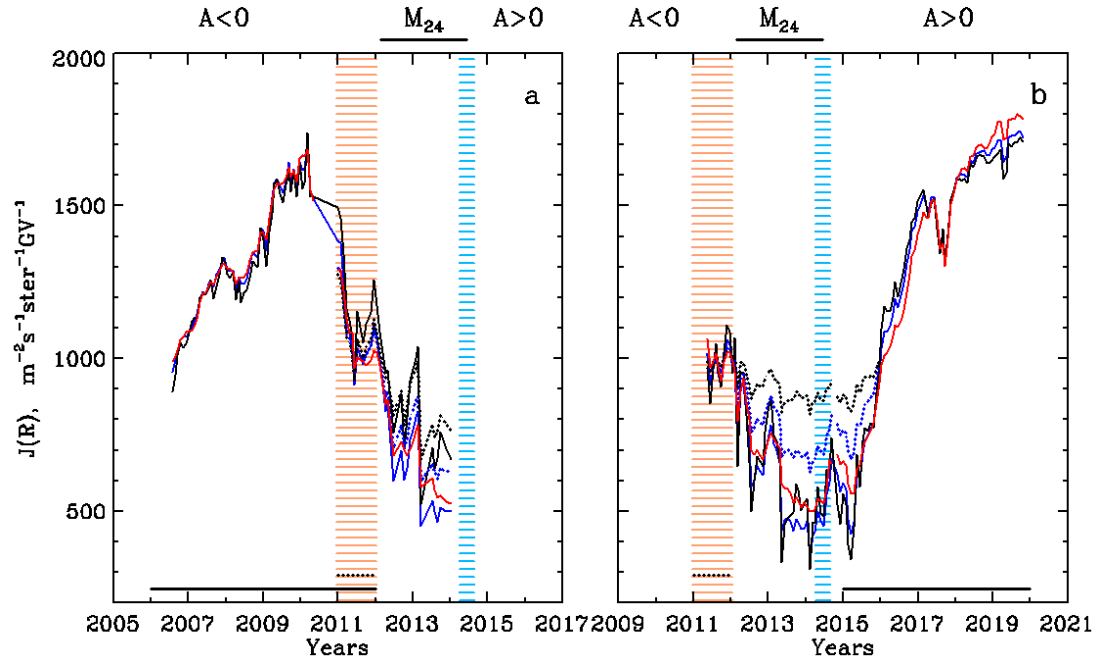

Figure 7. Change in the energy dependence of long-term GCR variations during HMF inversion in SC 24 in the intensity of protons of different energies as measured by PAMELA (*a*) and AMS-02 (*b*). The designations above the top panel and the hatched bands mean the same as in Figure 6. Red, blue, black solid and dotted lines are proton intensities in respectively 1–2, 2–3, 3–7.5 GV rigidity ranges, which are reduced to the intensity in the first of these ranges by linear regression to the time intervals indicated by solid and dotted lines near the time axis

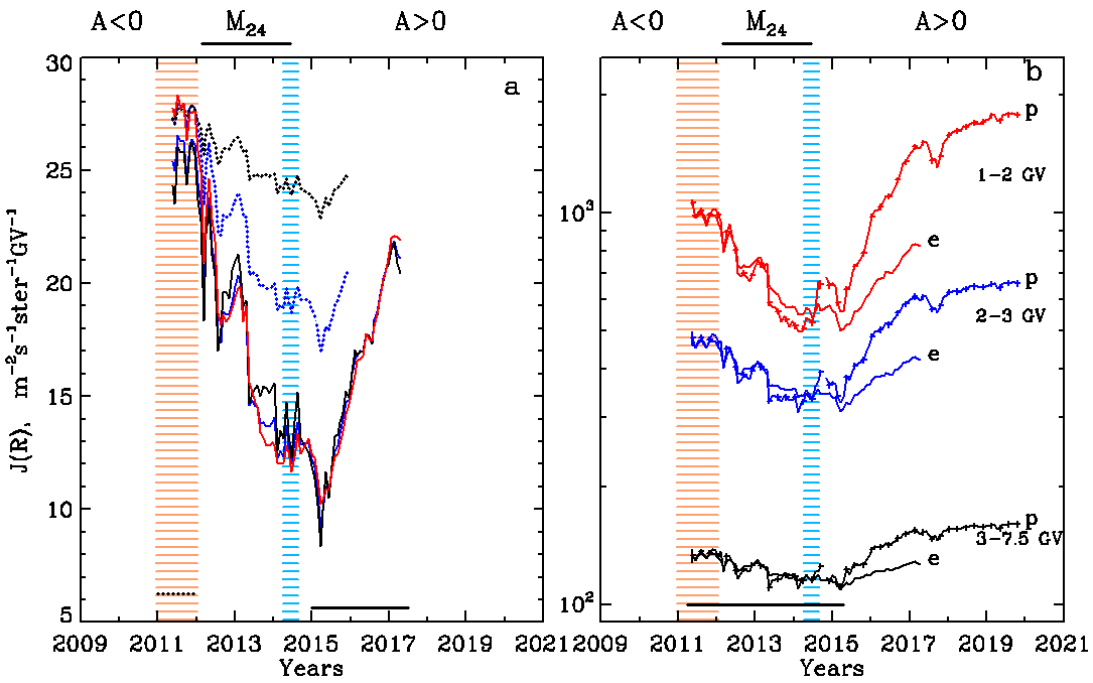

Figure 8. Change in the energy and charge dependences of long-term GCR variations during the HMF inversion in SC 24 in the intensity of protons and electrons of different energies as derived from AMS-02 data. Designations are the same as in Figure 7. Panel *a* is the same as in Figure 7, *b*, but for electrons. Panel *b* displays charge hysteresis during HMF inversion in SC 24. Red, blue, and black lines with symbols are proton intensities in the 1–2, 2–3, 3–7.5 GV rigidity ranges respectively; lines of the same color, but without symbols show the electron intensity in the same rigidity ranges, which is reduced to the proton intensity by linear regression in the time interval indicated by the straight line near the time axis

In Figure 8, *b*, proton intensities obtained from AMS-02 data [Aguilar et al., 2021] in the 1–2, 2–3, 3–7.5 GV rigidity ranges averaged over Bartels rotations in 05.2011–2019 are compared with electron intensities [Aguilar et al., 2018] in the same ranges for 05.2011–2017 after reducing them to proton intensities for a period close to the HMF inversion period (N=53). Correlation coefficients ρ=0.95±0.01, 0.93±0.02, 0.90±0.03. After the end of the HMF inversion in 2015–2016, the proton intensity is seen to recover at a rate much higher than the reduced electron intensity. We call the effect of significantly different rates of recovery of proton intensity and reduced electron intensity for all the rigidity ranges under study the charge dependence of long-term GCR variations after HMF inversion and consider it as the third effect in GCR intensity behavior associated with HMF inversion.

In the behavior of GCR intensity as derived from RBM and NM data (see Figure 1, *e*; Figures 2–5), significant variations during most HMF inversion periods can be seen approximately in antiphase with variations in the sunspot area and HMF intensity visible in Figure 1, *a*, *d*. In PAMELA and AMS-02 data (see Figures 6–8), there are also significant variations in the intensity of both protons and electrons during the HMF inversion in SC 24. In [Astaf'eva et al., 1997; Bazilevskaya et al., 1998; Storini et al., 2003], these variations are attributed to the so-called Gnevyshev effect, observed for the first time as a sharp weakening of solar activity and characteristics of solar cosmic ray flares during SC maxima [Gnevyshev, 1967]. As a result, there are two peaks with a dip between them in these characteristics. Accordingly, two dips with a peak in between are formed in the GCR intensity. Note that in the GCR intensity the Gnevyshev effect is observed not only in long-term, but also in shorter-period variations (in day-to-day variations, in 27-day variations) [Bazilevskaya et al., 1998]. In a number of papers [Krainev et al., 1999, 2015], we have assumed that this effect is due to the HMF inversion during this period, and consider the Gnevyshev effect as the fourth effect in GCR intensity behavior associated with HMF inversion.

3. DISCUSSION

Since the 1970s, a lot of observational, theoretical, and computational works have been devoted to the study of 22-year effects in GCR intensity (see [Potgieter, 2013] and references therein), but most attention has been concentrated on the periods of medium and low sunspot activity. It must have been assumed that during these periods the 22-year effects in the GCR intensity should be maximum, and during periods of maximum sunspot activity with the strongest and most disturbed HMF the change in the polarity of its regular component during the short phase of the HMF inversion per se (about a year) should not play a big role in long-term GCR variations.

In this paper, firstly we extend the time period in which the phenomena in the GCR intensity associated with HMF inversion are investigated. As it is clear from the previous section, the first and third effects in the GCR intensity, which we associate with the HMF inversion, refer to the rate of intensity recovery during about two-year period after the end of the HMF inversion last

phase. The first effect consists in the dependence of the rate of intensity recovery during this period for particles of the same charge on HMF inversion type ($dA/dt>0$ or $dA/dt<0$). The third effect, on the contrary, implies the particle charge dependence of the rate of intensity recovery during the same period after the end of the HMF inversion of the same type. Recall that despite its being outside of all three HMF inversion phases the above two-year period belongs to the SC interval with a high degree of HCS waviness (quasi-tilt α_{qt} >30°), when, according to the results of GCR intensity simulation, the influence of the 22-year cyclicity factors (primarily magnetic drift of particles) is insignificant compared to diffusion [Potgieter, 2013]. As already mentioned, we believe that heliospheric processes, including the GCR intensity modulation, are affected during this time period by HMF inversion details rather than by the degree of HCS waviness. At the same time, it is clear that phenomena in the time interval of interest are important for understanding the behavior of GCR intensity during SC. For example, when discussing the shape of the time intensity profile depending on the overall HMF polarity A, by acute-angled and plateau-shaped cycles is meant only part of the cycles around SC minimum. In general, for particles with a charge q during periods $qA>0$, the plateau-shaped part of the time profile, when the GCR intensity varies little with time, is preceded by an interval of a very rapid intensity increase, and during periods $qA<0$, the acute-angled part of the time profile, when the GCR intensity increases to maximum values, is preceded by an interval with approximately the same rate of intensity increase. In both cases, the behavior of the intensity during these periods of relatively high solar activity and degree of HCS waviness ($\alpha_{qt}>30°$) is conditioned by the processes we attribute to the previous HMF inversion.

Secondly, we believe that although during maximum sunspot activity and HMF inversion its intensity is on average significantly higher than during SC minima, regular HMF is topologically still determined by poloidal SMFs and the inversion of the latter should manifest itself at least in short-term decreases in the HMF strength. These manifestations of HMF inversion include the Gnevyshev effect in the sunspot activity level and HMF intensity (Figure 1, *a* and *d*), and the corresponding GCR intensity variations (approximately in antiphase with S_{ss} and B^{hmf}) clearly seen in Figure 1, *e*, as well as in different formats in Figures 2–8. We assign these GCR intensity variations to the fourth effect related to HMF inversion. Finally, the HMF strength variations caused by the Gnevyshev effect should lead to variations in kinetic characteristics — first of all, the diffusion coefficients and the magnetic drift velocity of particles of different energies, which should be manifested in violation of energy dependences of long-term GCR variations. We have discussed this phenomenon above as a sharp change in the energy dependence of long-term GCR variations and consider it as the second GCR intensity effect associated with HMF inversion.

As for the GCR intensity effects, formulated in the previous section, which we associate with HMF inversion, we would like to note first the qualitative nature of the formulations. The quantitative characteristics of each of the effects vary significantly from cycle to cycle and depend on the GCR intensity data series selected for analysis. We see two main reasons for this situation. First of all, solar cycles really differ greatly. The second reason is related to the properties of available data series. Of the six HMF inversions that occurred during the regular GCR monitoring the first five (at maxima of SC 19–23) were observed mainly in ground-based experiments on measurements of energy-integrated mixture of primary and secondary particles, generated in the atmosphere by a GCR nuclear component, as well as on extraterrestrial measurements of primary GCRs of significantly shorter duration in relatively narrow energy ranges. During the last HMF inversion (during maximum of SC 24, 2011–2014), the PAMELA and AMS-02 experiments opened up an opportunity to study the behavior of the differential intensity of particles of different types and charge. However, due to the imperfect arrangement of the periods of available PAMELA and AMS-02 data relative to the HMF inversion period, relationships between some intensity characteristics have to be studied using short series. But it is difficult to judge the significance of the correlation coefficients by their error, calculated as $\delta\rho=(1-p^2)/(N-1)^{0.5}$, at a short length of the compared series (for example, $N=9$ or $N=12$), and a more rigorous analysis is required to draw conclusions about the reliability of the correlation found between these series (see [Fisher, 1958]). If due to AMS-02 the possibility of studying the behavior of the differential intensity of particles of different types and charges still exists for the next 2–3 years, for the current period of HMF inversion in SC 25, which began at the end of 2022, we can hope that the formulated effects will be detailed and possibly corrected.

Because of the complex relationships in the Sun—heliosphere—GCR system, there is no complete agreement even among the authors of this article on the question of what causes some GCR intensity effects we associate with HMF inversion. In Section 2, the first effect in the behavior of GCR intensity during HMF inversion is formulated as a significant difference in the rate of intensity recovery after HMF inversions with $dA/dt>0$ and $dA/dt<0$. Nonetheless, the very fact of a good description of the time profile of GCR proton intensity by expressions (1), (2) in periods $A<0$ (this acute-angled profile is usually attributed to the dependence of intensity on the degree of HCS waviness α_{qt} [Jokipii, Thomas, 1981]) may be due to the dependence of α_{qt} on sunspot activity level and sunspot latitude (see [Bazilevskaya et al., 1995]). Moreover, we assume that the indicated difference in the rate of intensity recovery after HMF inversion in successive cycles is determined by the mechanisms that are well-known and usually involved in analysis (first of all, magnetic drift of particles), and the dependence of the recovery rate on particle charge (the third effect in our list) seems to confirm this. However, for more than fifty years there has been a viewpoint that the mode of reconnection between the heliospheric and galactic fields, which can additionally affect the rate of

intensity recovery after HMF inversion, depends on the overall HMF polarity [Schatten, Wilcox, 1969; Nagashima, 1977; Stozhkov et al., 2022]. Finally, although in Section 2 we associate the Gnevyshev effect in GCR intensity (the fourth effect in our list) with HMF inversion, analysis of various solar, heliospheric, and geophysical data suggests that the Gnevyshev effect may be a manifestation of a quasi-two-year variation in solar activity [Vecchio et al., 2010; Bazilevskaya et al., 2015; Adriani et al., 2018]. Note also that the quasi-two-year-type GCR intensity variations or the Gnevyshev effect are sometimes associated with global variations in HMF strength [Cane et al., 1999], which is close to our understanding of the Gnevyshev effect, or with the formation of barriers with enhanced HMF on the periphery of the heliosphere, which are formed when several coronal mass ejections merge [Potgieter, Le Roux, 1989].

Considering all four effects that we relate to HMF inversion allows us to combine them into two pairs. The first and third effects are intended to describe the rate of intensity recovery after inversion at SC maximum; the first effect can be formulated as a dependence of this rate on the sign of the overall HMF polarity A during the period after inversion (or on the dA/dt sign for HMF inversion) for particles with the same particle charge; the second, as a dependence of the intensity recovery rate on particle charge for the same dA/dt sign for HMF inversion. At least qualitatively these two effects can be formulated as a dependence of the intensity recovery rate after HMF inversion on the qA sign in the period after HMF inversion or the qdA/dt sign for HMF inversion. Note, however, that the dependence of the intensity recovery rate after SC maximum and HMF inversion on particle charge has been reliably observed so far only for SC 24. It is therefore desirable to test this regularity on the behavior of differently charged particles, recorded, for example, with high statistical accuracy in the AMS-02 experiment, during the period including the inversion in SC 25 and two years after it.

The second and fourth effects that we associate with HMF inversion represent the HMF inversion period per se, and a sharp change in the energy dependence of GCR intensity variation may be related to a variation in the regular HMF strength due to the Gnevyshev effect in this characteristic [Krainev, 1983; Krainev et al., 1984; Krainev et al., 1983a, b, 2015]. This assumption is supported by the fact that in the first approximation the intensity behavior during this period is the same for protons and electrons (see Figures 6 and 8, *b* and [Burger, Swanenburg, 1973]). Note, however, that the status of these two effects under discussion (a sharp change in the energy dependence of the GCR intensity variation and the Gnevyshev effect in this intensity) is different. If the Gnevyshev effect, i.e. significant intensity variations approximately in antiphase with variations in the sunspot area and the HMF strength, is observed for almost all the HMF inversion periods considered above, a sharp change in the energy dependence of the GCR intensity variation is clearly seen only for the HMF inversion periods in SC 20 and to a lesser extent in SC 24.

Note that such a representation of the GCR intensity effects associated with HMF inversion fits the scheme of two consecutive phenomena in GCRs during this period, which we have proposed earlier in [Krainev, 1983; Krainev et al., 1984; Krainev et al., 1983a, b; Krainev et al., 1985], when there were still no systematic measurements of electron intensity (other than those given in [Burger, Swanenburg, 1973]). We have assumed that the first of these phenomena does not depend on HMF inversion type and particle charge, and the second depends on dA/dt sign. Now, having much more reliable data on electron intensity [Aguilar et al., 2018], we can conclude that the second phenomenon depends on qdA/dt sign. In [Krainev et al., 2015], the first phenomenon was associated with the Gnevyshev effect; it was noted that both phenomena have a 22-year periodicity, i.e. they are well manifested during HMF inversion with $dA/dt>0$, i.e. in SC 20, 22, 24. This conclusion was, however, made by extrapolating the regression relationship between the count rates derived from RBM and Moscow NM data, which was determined for a narrow regression interval (1–2 years), to an HMF inversion period. It is not yet clear why in determining this regression relationship between successive HMF inversions over the entire interval, as has been done in Section 2, all these phenomena are most pronounced only in the first and last HMF inversions (in SC 20 and 24).

Detailing the behavior of HMF intensity during the inversion periods of the last five cycles with identification of individual effects, the results of which are reported in this paper, differs significantly from the approaches adopted by other researchers (see, e.g., [Aslam et al., 2023]). This may just be due to our interest in this particular SC phase since the very discovery of the first manifestation of the 22-year solar cyclicity in GCR intensity fifty years ago [Charakhchyan et al., 1973].

We are grateful to all the teams of researchers who present their results on the Internet. The discussion with Yu.I. Stozhkov, one of the main authors of the first detection of 22-year effects in GCR intensity, was useful and interesting. Mikhailov V.V. acknowledges the support from the Ministry of Science and Higher Education of the Russian Federation (Government assignment, Project “Fundamental and Applied Research of Cosmic Rays”, No. FSWU-2023-0068).

REFERENCES

Adriani O., Barbarino G.C., Bazilevskaya G.A., Bellotti R., Boezio M., Bogomolov E.A., et al. (PAMELA collaboration). Time dependence of the proton flux measured by PAMELA during the 2006 July–2009 December solar minimum. *Astrophys. J.* 2013, vol. 765, no. 2, p. 91. DOI: 10.1088/0004-637X/765/2/91.

Adriani O., Barbarino G.C., Bazilevskaya G.A., Bellotti R., Boezio M., Bogomolov E.A., et al. (PAMELA collaboration). Unexpected cyclic behavior in cosmic-ray protons observed by PAMELA at 1 au. *Astrophys. J. Lett*. 2018, vol. 852, no.2, p. L28. DOI: 10.3847/2041-8213/aaa403.

Aguilar M., et al. (AMS Collaboration). Observation of complex time structures in the cosmic-ray electron and positron fluxes with the Alpha Magnetic Spectrometer on the International Space Station. *Phys. Rev. Lett*. 2018, vol. 121, 051102.

Aguilar M., et al. (AMS Collaboration). Periodicities in the daily proton fluxes from 2011 to 2019 measured by the Alpha Magnetic Spectrometer on the International Space Station from 1 to 100 GV. *Phys. Rev. Lett*. 2021, vol. 127, 271102. DOI: 10.1103/PhysRevLett.127.271102.

Ahluwalia H.S. Eleven year variation of cosmic ray intensity and solar polar field reversals. *Proc. 16th International Cosmic Ray Conference.* 1979, vol. 12, p. 182–186.

Altschuler M.D., Newkirk G., Jr. Magnetic fields and the structure of the solar corona. I. Methods of calculating coronal fields. *Solar Phys*. 1969, vol. 9, pp. 131–149. DOI: 10.1007/BF00145734

Aslam O.P.M., Luo Xi, Potgieter M.S., Ngobeni M.D., Song Xiaojian. Unfolding drift effects for cosmic rays over the period of the Sun's magnetic field reversal. *Astrophys. J*. 2023, vol. 947, iss. 2, id. 72, 17 p. DOI: 10.3847/1538-4357/acc24a.

Astaf'eva N.M., Bazilevskaya G.A., Krainev M.B., Sladkova A.I. Depression in cosmic ray variations during the inversions of the polar magnetic field of the Sun. *Proc. 25th International Cosmic Ray Conference.* 1997, vol. 7, pp. 337–340.

Babcock H.D. The Sun's polar magnetic field. *Astrophysical Journal*. 1959. vol. 130, p. 364-365. DOI: 10.1086/146726.

Babcock H.W. The topology of the Sun's magnetic field and the 22-year cycle. *Astrophys. J*. 1961, vol. 133, p. 572. DOI: 10.1086/147060.

Bazilevskaya G.A., Svirzhevskaya A.K. On the stratospheric measurements of cosmic rays. *Space Sci. Rev.* 1998, vol. 85, pp. 431–521.

Bazilevskaya G.A., Krainev M.B., Makhmutov V.S., Stozhkov Yu.I., Svirzhevskaya A.K., Svirzhevsky N.S. The relationship between the galactic cosmic ray intensity and the sunspot distribution. *Adv. Space Res*. 1995, vol. 16, no. 9, pp. (9)221–(9)225. DOI: 10.1016/0273-1177(95)00339-G.

Bazilevskaya G., Krainev M., Makhmutov V., Sladkova A., Storini M., Fluckiger E. The Gnevyshev gap in cosmic ray physics. *Proc. 16th European Cosmic Ray Symposium*. 1998, pp. 83–86.

Bazilevskaya G., Broomhall A.-M., Elsworth Y., Nakariakov, V.M. A combined analysis of the observational aspects of the quasi-biennial oscillation in solar magnetic activity. *Space Sci. Ser. ISSI*. 2015, vol. 53, p. 359. DOI: 10.1007/978-1-4939-2584-1_12.

Bieber J.W., Evenson P.A., Matthaeus W.H. The nuts and bolts of cosmic ray modulation. *Proc. the 20th International Cosmic Ray Conference*. 1987, vol. 3, p. 175.

Burger J.J., Swanenburg B.N. Energy dependent time lag in the long-term modulation of cosmic rays. *J. Geophys. Res*. 1973, vol. 78, iss. 1, p. 292. DOI: 10.1029/JA078i001p00292.

Burton M.E., Crooker N.U., Siscoe G.L., Smith E.J. A test of source-surface models predictions of heliospheric current sheet inclination. *J. Geophys. Res*. 1994, vol. 99, iss. A1, pp. 1–10. DOI: 10.1029/93JA02100.

Cane H.V., Wibberenz G., Richardson I.G. von Rosenvinge T.T. Cosmic ray modulation and the solar magnetic field. *Geophys. Res. Lett*. 1999, vol. 26, pp. 565–568. DOI: 10.1029/1999GL900032

Charakhchyan A.N., Stozhkov Yu.I., Svirzhevsky N.S., Charakhchyan T.N. Anomalous effect in the 11-year galactic cosmic ray modulation. *Proc. the 13th International Cosmic Ray Conference.* 1973, vol. 2, pp. 1159–1164.

Charbonneau P. Dynamo models of the solar cycle. *Living Reviews Solar Physics.* 2010, vol. 7, p. 3. DOI: 10.1007/s41116-020-00025-6.

Evenson P., Garcia-Munoz M., Meyer P., Pyle K.R., Simpson J.A. A quantitative test of solar modulation theory: The proton, helium and electron spectra from 1965 through 1979. *Astrophys. J. Lett.* 1983, vol. 275, p. L15. DOI: 10.1086/184162.

Fisher R.A. Statistical methods for research workers. Oliver and Bold, 1954.

Forbush S.E. World-wide changes in cosmic-ray intensity. *Reviews of Modern Physics*. 1939, vol. 11, iss. 3-4, pp. 168–172. DOI: 10.1103/RevModPhys.11.168.

Forbush S.E. World-wide cosmic-ray variations, 1937–1952. *J. Geophys. Res*. 1954, vol. 59, iss. 4, pp. 525–542. DOI: 10.1029/JZ059i004p00525.

Forbush S.E. Variation with a period of two solar cycles in the cosmic-ray diurnal anisotropy and the superposed variations correlated with magnetic activity. *J. Geophys. Res*. 1969, vol. 74, iss. 14, p. 3451. DOI: 10.1029/JA074i014p03451.

Garcia-Munoz M., Meyer P., Pyle K.R., Simpson J.A., Evenson P. The dependence of solar modulation on the sign of the cosmic ray particle charge. *J. Geophys. Res*. 1986, vol. 91, no. A3, pp. 2858–2866. DOI: 10.1029/JA091iA03p02858.

Gnevyshev M.N. On the 11-year cycle of solar activity. *Solar Phys.* 1967, vol. 1, pp. 107–120. DOI: 10.1007/BF00150306.

Hale G.E. On the probable existence of a magnetic field in sun-spots. *Astrophys. J*. 1908, vol. 28, pp. 3015–343.

Hale G.E. Preliminary results of an attempt to detect the general magnetic field of the Sun. *Astrophys. J*. 1913, vol. 38, pp. 27-98.

Hale G.E., Ellerman F., Nicholson S.B., Joy A.H. The magnetic polarity of the sun-spots. *Astrophys. J*. 1919, vol. 49, pp. 153–178.

Howard R. Studies of solar magnetic fields. I. The average field strengths. *Solar Phys*. 1974, vol. 38, pp. 283–299. DOI: 10.1007/BF00155067.

Jokipii J.R., Levy E.H. Electric field effects on galactic cosmic rays at the heliospheric boundary. *Proc. 16th International Cosmic Ray Conference*. 1979, vol. 3, pp. 52–56.

Jokipii J.R., Thomas B. Effect of drift on the transport of cosmic rays. IV. Modulation by a wavy interplanetary current sheet. *Astrophys. J*. 1981, vol. 243, pp. 1115–1122. DOI: 10.1086/158675.

Jokipii J.R., Levy E.H., Hubbard W.B. Effects of particle drift on cosmic-ray transport. I. General properties, application to solar modulation. *Astrophys. J*. 1977, vol. 213, pp. 861–868. DOI: 10.1086/155218.

Krainev M.B. The solar corona expansion geometry and cosmic ray effects. IV. On the cosmic ray energy change due to the electric field. *Proc. 16th International Cosmic Ray Conference.* 1979, vol. 3, pp. 236–241.

Krainev M.B. Influence of the general magnetic field of the Sun on the 11-year cycle and "anomalous" phenomena in galactic cosmic rays. *Izvestiia Akademii Nauk SSSR, Seriia Fizicheskaia* [Bulletin of the Russian Academy of Sciences: Physics]. 1983, vol. 47, no 9, pp. 1754–1760. (In Russian).

Krainev M.B. Manifestations of two branches of solar activity in the heliosphere and GCR intensity. *Solar-Terr. Phys.* 2019, vol. 5, iss. 4, pp. 10–20. DOI: 10.12737/stp-54201902.

Krainev M.B., Kalinin M.S. On the GCR intensity and the inversion of the heliospheric magnetic field during the periods of the high solar activity. *Proc. 33rd International Cosmic Ray Conference.* 2014, icrc2013-0317/1-4, ArXiv:1411.7532 [astro-ph.SR].

Krainev M.B., Stozhkov Yu.I., Charakhchyan T.N. On the energetic "hysteresis" in the galactic cosmic ray intensity. *Proc. 18th International Cosmic Ray Conference*. 1983a, vol. 3, pp. 23–26.

Krainev M.B., Stozhkov Yu.I., Charakhchyan T.N. On the "anomalous" phenomena in the galactic cosmic ray intensity in the periods of the inversion of general magnetic field of the Sun. *Proc. 18th International Cosmic Ray Conference*. 1983b, vol. 3, pp. 95–98.

Krainev M.B. Stozhkov Yu.I., Charakhchyan T.N. Galactic cosmic rays during periods of solar-magnetic-field inversion. *Izvestiia Akademii Nauk SSSR, Seriia Fizicheskaia* [Bulletin of the Russian Academy of Sciences: Physics]. 1984, vol.48, no 11, pp. 2100–2102. (In Russian).

Krainev M.B. Stozhkov Yu.I., Charakhchyan T.N. On the influence of the heliomagnetospheric periphery on the galactic cosmic rays. *Proc. 19th International Cosmic Ray Conference*. 1985, vol. 4, pp. 481–484.

Krainev M.B., Storini M., Bazilevskaya G.A., Fluckiger E.O., Makhmutov V.S., Sladkova A.I., Starodubtsev S.A. The Gnevyshev gap effect in galactic cosmic rays. *Proc. 26th International Cosmic Ray Conference*. 1999, vol. 7, pp. 155–158.

Krainev M., Bazilevskaya G., Kalinin M., et al. GCR intensity during the sunspot maximum phase and the inversion of the heliospheric magnetic field. *Proc. Science*. 2015. PoS (ICRC2015) 081/1-8.

Krymskiy G. F. Diffusion mechanism of diurnal cosmic-ray variations. *Geomagnetizm i Aeronomiya* [Geomagnetism and Aeronomy]. 1964, vol. 4, pp. 763–769.

Lockwood J.A., Leznyak J.A., Webber W.R. Change in the eleven-year modulation at the time of the June 8, 1969, Forbush decrease. *J. Geophys. Res*. 1972, vol. 77, iss. 25, p. 4839. DOI: 10.1029/JA077i025p04839.

Martucci M., Munini R., Boezio M., Di Felice V., Adriani O, et al. (PAMELA collaboration). Proton fluxes measured by the PAMELA experiment from the minimum to the maximum solar activity for solar cycle 24. *Astrophys. J. Lett*. 2018, vol. 854, p. L2. DOI: 10.3847/2041-8213/aaa9b2.

Nagashima K. Long term modulation of cosmic rays in helio-magnetosphere. *Proc. 15th International Cosmic Ray Conference*. 1977, vol. 10, pp. 380–396.

Parker E.N. Cosmic ray modulation by solar wind. *Phys. Rev*. 1958, vol. 110, p. 1445. DOI: 10.1103/PhysRev.110.1445.

Parker E.N. Interplanetary dynamical processes. 1963. New York. Interscience Publishers.

Parker E.N. The passage of energetic charged particles through interplanetary space. *Planetary and Space Sciences*. 1965, vol. 13, pp. 9–49. DOI: 10.1016/0032-0633(65)90131-5.

Potgieter M.S. Solar modulation of cosmic rays. *Living Reviews. Solar Physics*. 2013, vol. 10, p. 3. DOI: 10.12942/lrsp-2013-3.

Potgieter M. S., Le Roux J.A. More on a possible modulation barrier in the outer heliosphere. *Adv. Space Res*. 1989, vol. 91, p. 121. DOI: 10.1016/0273-1177(89)90318-9.

Schatten K.H., Wilcox J.M. Direction of the nearby galactic magnetic field inferred from a cosmic-ray diurnal anisotropy. *J. Geophys. Res.* 1969, vol. 74, iss. 16, p. 4157. DOI: 10.1029/ JA074i016p04157.

Schatten K.H., Wilcox J.M., Ness F.N. A model of interplanetary and coronal magnetic fields. *Solar Phys*. 1969, vol. 6, pp. 442–455.

Sheeley N.R., Jr. Polar faculae during the interval 1906–1975. *J. Geophys. Res*. 1976, vol. 81, p. 3462. DOI: 10.1029/ JA081i019p03462.

Sheeley N.R., Jr. A century of polar faculae variations. *Astrophys. J*. 2008, vol. 680, pp. 1553–1559. DOI: 10.1086/588251.

Shulz M. Interplanetary sector structure and the heliomagnetic equator. *Astrophys. Space Sci*. 1973, vol. 24, p. 371. DOI: 10.1007/BF02637162.

Simpson J.A. The primary cosmic ray spectrum and the transition region between interplanetary and interstellar space. *Proc. 8th International Cosmic Ray Conference*. 1963, vol. 2, p. 155.

Simpson J.A. Cosmic ray astrophysics at Chicago (1947–1960). *Astrophys. Space Sci. Library*. 1985, vol. 118, p. 385. DOI: 10.1007/978-94-009-5434-2_36.

Simpson J.A. The cosmic ray nucleonic component: The invention and scientific uses of the neutron monitor, cosmic rays and Earth. *Space Sci. Ser. ISSI*. 2000, vol. 10, pp. 11–32. DOI: 10.1007/978-94-017-1187-6_2.

Smith E.J. The heliospheric current sheet. *J. Geophys. Res*. 2001, vol. 106, iss. A8, pp. 15819–15832. DOI: 10.1029/2000 JA000120.

Smith E.J. Solar cycle evolution of the heliospheric magnetic field: The Ulysses legacy. *J. Atmos. Solar-Terr. Phys*. 2011, vol. 73, iss. 2-3, pp. 277–289. DOI: 10.1016/j.jastp.2010.03.019.

Storini M., Bazilevskaya G.A., Fluckiger E.O., Krainev M.B., Makhmutov V.S., Sladkova A.I. The Gnevyshev gap: A review for space weather. *Adv. Space Res*. 2003, vol. 31, no. 4, pp. 895–900. DOI: 10.1016/S0273-1177(02)00789-5.

Stozhkov Yu.I., Charakhchyan T.N. 11-year modulation of cosmic ray intensity and distribution of spots in heliographic latitude. *Geomagnetizm i Aeronomiya* [Geomagnetism and Aeronomy]. 1969, vol. 9, no. 5, pp. 803–808. (In Russian).

Stozhkov Yu.I., Charakhchyan T.N. On the role of the heliolatitudes of sunspots in the 11-year galactic cosmic ray modulation. *Acta Phys. Acad. Sci*. Hungaricae. 1970, vol. 29, suppl. 2, pp. 301–304.

Stozhkov Yu.I., Svirzhevsky N.S., Bazilevskaya G.A., Svirzhevskaya A.K., Kvashnin A.N., Krainev M.B., Makhmutov V.S., Klochkova T.N. Fluxes of cosmic rays in the maximum of absorption curve in the atmosphere and at the atmosphere boumdary (1957–2007). *Preprint 14, Lebedev Physical Institute, Moscow*. 2007, 77 p.

Stozhkov Yu.I., Svirzhevsky N.S., Bazilevskaya G.A., Kvashnin A.N., Makhmutov V.S., Svirzhevskaya, A.K. Long-term (50 years) measurements of cosmic ray fluxes in the atmosphere. *Adv. Space Res*. 2009, vol. 44, pp. 1124–1137. DOI: 10.1016/j.asr.2008.10.038.

Stozhkov Yu.I., Makhmutov V.S., Svirzhevsky N.S. About cosmic ray modulation in the heliosphere. *Universe*. 2022, vol. 8, iss.11, p. 558. DOI: 10.3390/universe8110558.

Svirzhevskaya A.K., Stozhkov Yu.I., Charakhchyan T.N. Anomalous effect in the spectrum of cosmic ray variations in 1971–1973. *Proc. 14th International Cosmic Ray Conference*. 1975, vol. 3, pp. 985–989.

Vecchio A., Laurenza M., Carbone V., Storini M. Quasi-biennial modulation of solar neutrino flux and solar and galactic cosmic rays by solar cyclic activity. *Astrophys. J. Lett*. 2010, vol. 709, pp. L1–L5. DOI: 10.1088/2041-8205/709/1/L1.

Zhao X., Hoeksema J.T. A coronal magnetic field model with horizontal volume and sheet currents. *Solar Phys*. 1994, vol. 151, pp. 91–104. DOI: 10.1007/BF00654084.

URL: ftp://ftp.swpc.noaa.gov/pub/forecasts/SRS (accessed October 14, 2023).

URL: http://wso.stanford.edu (accessed October 14, 2023).

URL: https://solarscience.msfc.nasa.gov (accessed October 14, 2023).

URL: ftp://omniweb.gsfc.nasa.gov/pub/data/omni/low_res_omni (accessed October 14, 2023).

URL: https://sites.lebedev.ru/en/DNS_FIAN (accessed October 14, 2023).

URL: http://www.nmdb.eu (accessed October 14, 2023).

Original Russian version: Krainev M.B., Bazilevskaya G.A., Kalinin M.S., Mikhailov V.V., Svirzhevskaya A.K., Svirzhevsky N.S., published in Solnechno-zemnaya fizika. 2023. Vol. 9. Iss. 4. P. 5–20. DOI: 10.12737/szf-94202301.

How to cite this article

Krainev M.B., Bazilevskaya G.A., Kalinin M.S., Mikhailov V.V., Svirzhevskaya A.K., Svirzhevsky N.S. Fifty years of studying the GCR intensity during inversion of heliospheric magnetic fields I. Observations. *Solar-Terrestrial Physics*. 2023. Vol. 9. Iss. 4. P. 3–16. DOI: 10.12737/stp-94202301.